Scattering Mechanisms in InN

Sibel Gökden*

Balikesir University, Department of Physics, Balıkesir, Turkey
(Received May 30, 2006)

The effect of scattering mechanisms on the published Hall electron mobility data has been investigated, in detail, as a function of temperature. The important mechanisms of electron scattering considered are those by charged dislocations, ionized impurities, polar optical phonons, and bulk acoustic phonons via deformation of the potential and piezoelectric fields. The results are discussed using a theoretical model that takes into account the most important scattering mechanisms within the framework of the Boltzmann transport equation. We show that the dominant contribution to the mobility is found to be from dislocations via the coulomb interaction at low temperatures. The mobility versus carrier density at room temperature for various dislocation densities has been plotted, and we estimated the dislocation density. The best fit to the experimental data is obtained for a dislocation density of $N_{dis} \cong 2.85 \times 10^{13} \mathrm{m}^{-2}$. The polar optical phonon scattering seems to dominate at high temperatures. The results were compared with the experimental data, and we found a reasonable correlation. Also the calculated mobility agrees reasonably well with the published Hall mobility calculated using the variational principle by Chin *et al.* [J. Appl. Phys. **75** 7365, (1994)].

PACS numbers: 72.80 Ey, 72.20.Fr, 61.72.Lk

I. INTRODUCTION

In recent years indium nitride (InN), as an important group III-V nitride semiconductor with many potential applications, has attracted much attention [1–3]. Besides its application for full color displays based on group-III nitride alloys, indium nitride is expected to be used for the fabrication of high performance high electron mobility transistors, since it will have a higher peak-drift velocity and higher peak overshoot velocity than GaN, with a large breakdown electric field and a wide band gap [4–6]. Because of the narrow band gap of 1.89 eV [7–9] at 300 K in wurtzite-InN, InN is potentially suitable as a nitride-based material for visible light-emitting diodes ranging from red to blue by alloying with wide-gap GaN and AlN. Recent progress in epitaxial growth techniques has led to the availability of high quality InN, where strong experimental evidence exists to show that the real band gap energy of InN is between 0.7 and 0.8 eV at room temperature [10].

High-quality InN films are difficult to prepare because the lattice mismatch and the mismatch of thermal expansion between the epitaxial film and substrate are very large. InN has been grown so far by various methods, such as reactive sputtering [11], metalorganic vapor phase epitaxy (MOVPE) [12, 13], hydride vapor phase epitaxy (HVPE), radiofrequency ion sputtering (rf-RIS) [14], microwave-excited MOVPE [15] and magnetron

sputtering [16]. Tansley and Foley reported on the high mobility of μ=2700 cm^2/V.s at room temperature for a carrier concentration in an InN sample grown by rf-RIS [14]. At present, even though there are more complicated and sophisticated growth techniques than those mentioned above, there are no new published reports better than the high mobilty and low carrier concentration results of Tansley and Foley. The samples produced with these improved methods result in electron concentrations in the mid-10^{18} cm^{-3} range, with room temperature electron mobilities well in excess of 1000 cm^2/V.s. [15, 16]. This value is less then half of that in the previous study.

There has been a growing activity, worldwide, for the determination of electrical and optical properties of InN [17]. Even though there are many experimental works on the Hall mobility measurements, there are scarcely any reports concerned with the effect of scattering mechanisms on the transport properties of InN [14].

This work is focused on calculating the effect of scattering mechanisms by using the Boltzman transport equation on the electron Hall mobility data published by Tansley and Foley [14]. The calculated values were also compared with the experimental data and the theoretical approach of the authors. A satisfactory agreement of the experimental data and the theoretical approach is obtained.

II. SCATTERING MECHANISMS

Here we describe the various scattering mechanisms which influence the Hall mobility. The dominant scattering mechanisms operative in bulk GaN has been investigated in detail [18].

In the low temperature region of interest, electrons are considered to be scattered by charged dislocations via the coulomb interaction and impurities. Dislocations in the layer/substrate interface region have a significant impact on the mechanical, electrical, and optical properties of these materials. The mismatches in the lattice constant and thermal expansion coefficient between InN and the substrate are expected to generate high densities of threading edge, screw, and mixed dislocations. Thus, the band extremes (conduction band minimum, valance band maximum) shift under the influence of the strain fields existing around the interface region. As a result, the imperfections which cause scattering of the electrons will affect the device function, lifetime, and efficiency. When a dopant is ionized to produce an extra free electron, the electron scatters from the ion. The scattering potential is Coulombic in nature, except that the potential is suppressed by screening effects. The screening is due to the presence of the other free electrons which form a cloud around the ion, so the effect of the potential is short range.

At intermediate temperatures, bulk acoustic phonons via the deformation potential and piezoelectric fields are the dominant scattering mechanisms. The vibrations of the atoms produce disturbing potentials that result in the scattering of electrons and cause spatial and temporal fluctuations in the conduction and valance band energies. The electrons (holes) then scatter from these disturbances. The phonon scattering also limits the performance of both electronic and optoelectronic devices.

Polar optical phonon scattering is the most important scattering mechanisms for the high field or high temperature transport of electrons. The optical phonons produce a potential disturbance which is proportional to the atomic vibration amplitude.

The analytical expressions for the above mentioned scattering mechanisms are briefly summarized below, and the material parameters used in the calculations are also listed in Table I.

TABLE I: Values of InN material constants used in the calculations.

Electron effective mass	$m^* = 0.14\mathrm{m}_0$ [25] $m^* = 0.04\mathrm{m}_0$ [26]
High frequency dielectric constant	$\varepsilon_\infty = 8.4$
Static dielectric constant	$\varepsilon_s = 15.3$
LO-phonon energy (meV)	$\hbar\omega = 73$
Deformation potential (eV)	$E_D = 7.1$
Net carrier concentration (m^{-3}) (T=40K)	$n = 5 \times 10^{22}$
Piezoelectric constants ($\mathrm{C/m}^2$)	$e_{15} = -0.22$ $e_{31} = -0.22$ $e_{33} = 0.43$
Elastic constants (10^{11} $\mathrm{N/m}^2$)	$c_{LA} = 1.82$ $c_{TA} = 0.099$
Electromechanical coupling coefficient	$K^2 = 0.028$
Lattice constants (Å)	$c_0 = 5.71$
Electron wavevector (m^{-1})	$k = 5.74 \times 10^8$
Dangling bonds (m)	$d = 2.4 \times 10^{-9}$

II-1. Dislocation Scattering

The model used to calculate the dislocation scattering takes into account that threading dislocations with an edge component act as Coulomb scattering centers [19, 20]. If dislocations have an edge component they introduce acceptor centers along the dislocation line, which capture electrons from the conduction band in an n-type semiconductor. The dislocation lines are negatively charged, and a space charge is formed around them which will scatter electrons traveling across the dislocations, thus reducing the mobility. The electron mobility due to such scattering by dislocations is given by the expression [20]

$$\mu_{dis} = \frac{30\sqrt{2\pi}\varepsilon_s d^2 (kT)^{3/2}}{N_{dis} e^3 f^2 \lambda_d \sqrt{m^*}}\,, \tag{1}$$

where d is the distance between acceptor centers along the dislocation line (dangling bonds), ε_s is the static permittivity, f is the occupation rate of the acceptor centers, N_{dis} is the density of dislocations, and λ_d is the Debye screening length,

$$\lambda = \left(\frac{\varepsilon_s k_{\mathbf{B}} T}{e^2 n}\right)^{1/2}, \tag{2}$$

where n is the net carrier concentration. Thus, according to Eqs. (1) and (2), the electron mobility due to scattering by dislocations should increase monotonically with net carrier concentration.

II-2. Impurity Scattering

Ionized impurity scattering usually dominates the mobility primarily at low temperatures. Impurity scattering occurs at particular scattering centers. This allows us to define a scattering cross-section in terms of the number of particles scattered in a particular direction relative to the incident particle flux. The cross-section may be found by setting up the Hamiltonian for the scattering potential and looking at the asymptotic solutions. Solutions may be found so that both the Conwell-Weisskopf and Brooks-Herring solutions are encompassed in the appropriate limits. It is an elastic process and represents an important source of momentum relaxation. Using the Brooks–Herring model, the mobility is given by [21]

$$\mu_{imp} = \frac{2^{7/2}(4\pi\varepsilon_s)^2 \left(k_B T\right)^{3/2}}{(m^*)^{1/2}\, \pi^{3/2} \mathrm{Z}^2 e^3 N_{imp} \left[\ln\left[1+\beta^2\right] - \frac{\beta^2}{1+\beta^2}\right]}, \tag{3}$$

where N_{imp} is the concentration of ionized impurity in the crystal, Z is the charge number of each ionized atom, and

$$\beta = 2\frac{m^*}{\hbar}\left(\frac{2}{m^*} 3 k_B T\right)^{1/2} \lambda_d \,. \tag{4}$$

Here we have assumed $Z = 1$.

II-3. Acoustic Phonon Scattering by a Deformation Potential

Because the short range distortions of the lattice cause changes in the potential due to mechanical stress, we can consider the scattering of electrons by bulk acoustic phonons via the deformation potential and piezoelectric effects. It has been assumed that the interaction can be described by a simple deformation potential statically screened. The mobility for acoustic phonons is given by [22]

$$\mu_{DP} = \frac{\pi\hbar^3 c_{LA} e}{E_D^2 k_B T m^{*2} k}\left[1 - \frac{q_s^2}{k^2} + \frac{q_s^4}{8k^4}\left(3\ln\left\{1 + (2k/q_s)^2\right\} - \frac{1}{1+(q_s/2k)^2}\right)\right]^{-1}, \tag{5}$$

where E_D is the deformation potential constant, k is the electron wave vector, c_{LA} is the angular average of the elastic constant describing the propagation of LA waves, and q_s is

the reciprocal screening length in 3D,

$$q_s^2 = -\frac{e^2}{\varepsilon_s}\int \frac{df^+(E)}{dE} N(E)\, d(E)\,. \tag{6}$$

Here $N(E)$ is the density of states function and $f(E)$ is the Fermi-Dirac function.

II-4. Piezoelectric Scattering

The strength of the interaction is determined by the dimensionless electromechanical coupling coefficient K. This quantity has contributions from both LA and TA phonons. The electromechanical coupling coefficient K is given by [23]

$$K^2 = \frac{\langle e_{LA}^2 \rangle}{\varepsilon_s c_{LA}} + \frac{\langle e_{TA}^2 \rangle}{\varepsilon_s c_{TA}}\,, \tag{7}$$

where c_{LA} and c_{TA} are angular averages of the elastic constants describing the propagation of LA and TA waves. The spherical averages of the effective constants for the LA and TA modes are

$$\begin{aligned} \langle e_{LA}^2 \rangle &= \tfrac{1}{105}\left[8\left(2e_{15}+e_{31}\right)^2 + 12\left(2e_{15}+e_{31}\right)e_{33} + 15e_{33}^2\right]\,, \\ \langle e_{TA}^2 \rangle &= \tfrac{1}{105}\left[6\left(e_{33}-e_{31}-e_{15}\right)^2 + 16\left(e_{33}-e_{31}-e_{15}\right)e_{15} + 48e_{15}^2\right]\,. \end{aligned} \tag{8}$$

Here e_i are the piezoelectric constants for the wurtzite structure. The mobility is given by [22]

$$\mu_{PE} = \frac{2\pi\varepsilon_s\hbar^3 k}{K^2 e k_B T m^{*2}}\left[1 - \frac{q_s^2}{k^2} + \frac{q_s^4}{8k^4}\left(3\ln\left\{1+\left(2k/q_s\right)^2\right\} - \frac{1}{1+\left(q_s/2k\right)^2}\right)\right]^{-1}. \tag{9}$$

II-5. Polar Optic Phonon Scattering

At high temperatures and high electron densities, it was found from solving the Boltzmann equation exactly that the mobility associated with LO scattering falls with increasing electron concentration [24]. For $E < \hbar\omega$ the momentum relaxation rate due to absorption is given by [22]

$$\begin{aligned} \tfrac{1}{\tau_{LO}} &= \omega_0\left[n\left(\omega\right)+1\right]\tfrac{f^+(E+\hbar\omega)}{f^+(E)}\left(\tfrac{\hbar\omega}{E}\right)^{1/2}\sinh^{-1}\left(\tfrac{E}{\hbar\omega}\right)^{1/2}, \\ \omega_0 &= \tfrac{e^2}{4\pi\hbar}\left(\tfrac{2m^*\omega}{\hbar}\right)^{1/2}\left(\tfrac{1}{\varepsilon_\infty}-\tfrac{1}{\varepsilon_s}\right)\,. \end{aligned} \tag{10}$$

where $\hbar\omega$ is the optical phonon energy and $n(\omega)$is the optical phonon occupation factor. ε_∞ is the high frequency dielectric constant.

Different scattering mechanisms have been considered for evaluating the mobility. The final value has been obtained using Matthiessen's rule:

$$\frac{1}{\mu} = \sum_i \frac{1}{\mu_i}\,, \tag{11}$$

where μ_i is the contribution due to the ith scattering mechanism characterized by a scattering time equal to τ_i, i.e., $\mu_i = e\tau_i/m^*$, with m^* being the electron effective mass.

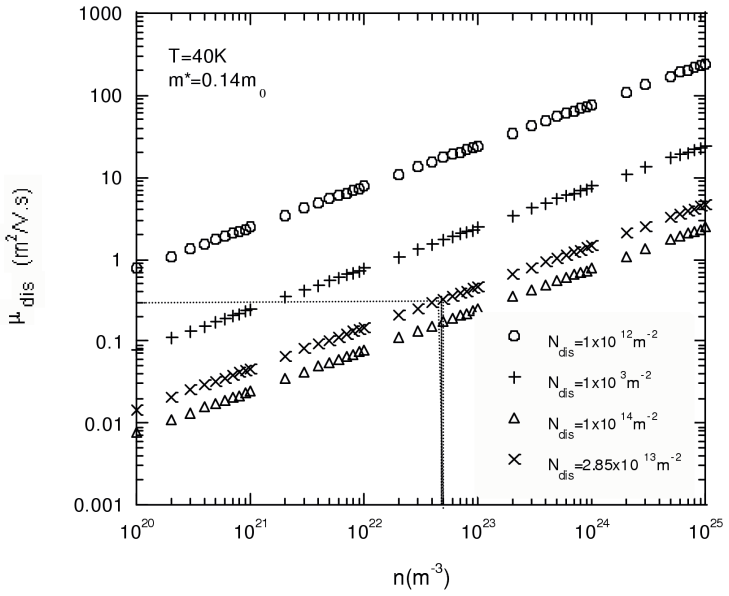

FIG. 1: Calculated electron mobility versus net carrier concentration for different values of N_{dis} at $T = 40$ K.

III. 3. RESULTS AND CONCLUSIONS

We plotted the mobility versus carrier density at $T = 40$ K for various dislocation densities in Fig. 1. Here we assumed that the mobility is solely determined by dislocation scattering. The best fit to the experimental data is obtained for a dislocation density of $N_{dis} = 2.85 \times 10^{13}$ m^{-2}.

In Figs. 2 and 3 we plot the temperature dependence of the experimental mobility together with the calculated mobility, where the contributions due to the individual scattering mechanisms and the total value, which was obtained using Matthiessen's rule, are shown. At high temperatures polar-optical phonon scattering is the mobility limiting process. Dislocation scattering seems to be dominant for low temperatures. The obtained theoretical results, using a model within the framework of the Boltzmann transport equation, are found to be in a good agreement with the experimental mobility data and the mobility data previously calculated using the variational principle (VP). The calculated results are found to agree reasonably well with the experimental Hall mobility data for both of the effective mass values, $m^* = 0.14$ m$_0$ and $m^* = 0.04$ m$_0$, which can be found in the literature.

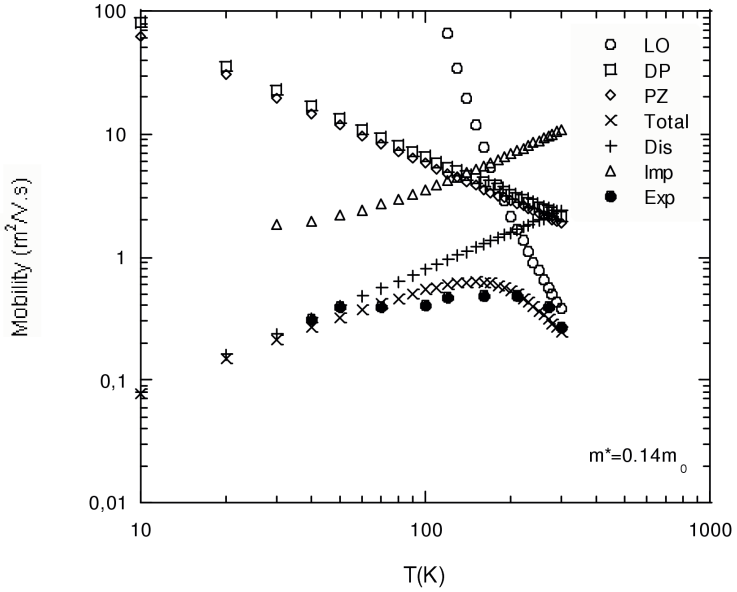

FIG. 2: Experimental and calculated mobility as a function of temperature for $m^* = 0.14$ m_0. LO: optical phonon scattering; DP: deformation potential scattering; PE: piezoelectric scattering; DIS: dislocation scattering; IMP: ionized impurity scattering; EXP: experimental values.

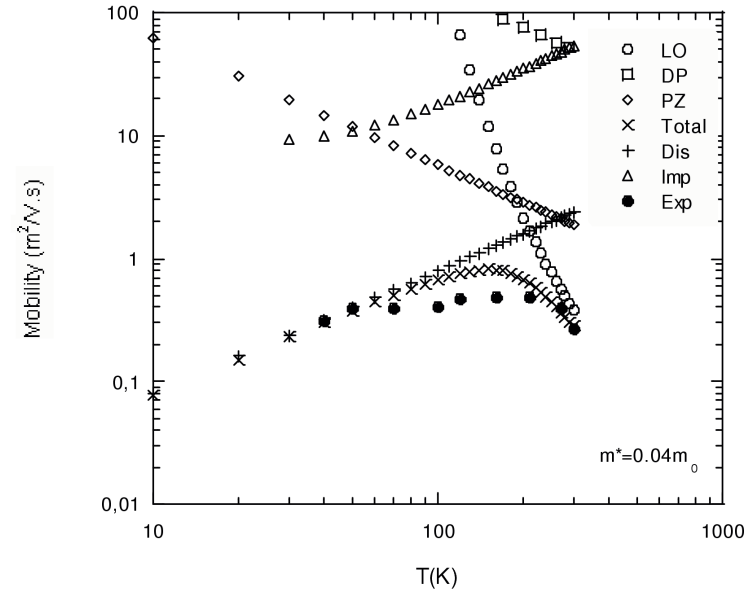

FIG. 3: Experimental and calculated mobility as a function of temperature for $m^* = 0.04$ m_0. LO: optical phonon scattering; DP: deformation potential scattering; PE: piezoelectric scattering; DIS: dislocation scattering; IMP: ionized impurity scattering; EXP: experimental values.

References

* Electronic address: sozalp@balikesir.edu.tr

[1] S. Yamagushi *et al.*, J. Appl. Phys. **85**, 7682 (1999).
[2] H. Lu *et al.*, Appl. Phys. Lett. **79**, 1489 (2001).
[3] M. Higashiwaki and T. Matsui, Jpn. J. Appl. Phys. **41**, L540 (2002).
[4] S. K. O'Leary, B. E. Foutz, M. S. Shur, U. V. Bhapkar, and L. F. Eastman, J. Appl. Phys. **83**, 826 (1997).
[5] E. Bellotti, B. K. Doshi, K. F. Brennan, J. D. Albrecht, and P. P. Ruden, J. Appl. Phys. **85**, 916 (1999).
[6] B. E. Foutz, S. K. O'Leary, M. S. Shur, and L. F. Eastman, J. Appl. Phys. **85**, 7727 (1999).
[7] J. Hovel and J. J. Cuomo, Appl. Phys. Lett. **20**, 71 (1972).
[8] K. Osamura, S. Nara, and Y. Murakami, J. Appl. Phys. **46**, 3432 (1975).
[9] A. Tyagai *et al.*, Sov. Phys. Semicond. **11**, 1257 (1977).
[10] S. Yamaguchi *et al.*, Appl. Phys. Lett. **76**, 876 (2000).
[11] K. Kubota, Y. Kobayashi, and K. Fujimoto, J. Appl. Phys. **66**, 2984 (1989).
[12] Q. X. Guo, T. Yamamura, A. Yoshida, and N. Itoh, J. Appl. Phys. **75**, 4927 (1994).
[13] Q. X. Guo, O. Kato, and A. Yoshida, J. Appl. Phys. **73**, 7969 (1993).
[14] T. L. Tansley and C. P. Foley, Electron. Lett. **20**, 1066 (1984).
[15] A. Wakahara, T. Tsuchiya, and A. Yoshida, J. Cryst. Growth **99**, 385 (1990).
[16] K. Kubota, Y. Kobayashi, and K. Fujimoto, J. Appl. Phys. **66**, 2984 (1989).
[17] D. C. Look, H. Lu, W. J. Schaff, J. Jasinski, and Z. Liliental-Weber, Appl. Phys. Lett. **80**, 258 (2002).
[18] D. C. Look and J. R. Sizelove, Phys. Rev. Lett. **82**, 1237 (1999).
[19] W. T. Read, Philos. Mag. **45**, 775 (1954).
[20] B. Pödör, Phys. Stat. Solid. **16**, K167 (1966).
[21] J. D. Wiley, in *Semiconductors and Semimetals* (Vol.10), eds. R. K. Wilardson and A.C. Beer (Academic, Newyork, 1975), pp 91–174.
[22] B. K. Ridley, B. E. Foutz, and L. F. Eastman, Phys. Rev. B **61**, 16862 (2000).
[23] A. R. Hutson, J. Appl. Phys. **32**, 2287 (1961).
[24] B. K. Ridley, J. Appl. Phys. **84**, 4020 (1998).
[25] A. Kasic, M. Schubert, Y. Saito, Y. Nanishi, and G. Wagner, Phys. Rev. B **65**, 115206 (2002).
[26] T. Unishima, M Higashiwaki, and T. Matsui, Phys. Rev. B **68**, 235204 (2003).